

Extinguishment of Liquid Heptane and Gaseous Propane Diffusion Flames

M. Babb,* S. R. Gollahalli,† and C. M. Sliepcevich‡
University of Oklahoma, Norman, Oklahoma, 73019

This paper presents a comparative study of the extinguishment of liquid heptane and gaseous propane diffusion flames caused by the addition of flame-suppressing agents (N_2 and CO_2) into a coflowing stream of air. Measurements included mass burning rate, concentrations of suppressants at flame extinction, in-flame temperature profiles, and exhaust composition. Adiabatic equilibrium temperatures of the stoichiometric mixtures of the fuels in pure airstream, and in the airstream containing flame suppressants with the concentrations corresponding to flame extinction, were calculated. Although the extinction processes of liquid and gaseous fuel flames are markedly different, even when both are buoyancy dominated, the extinction mechanism of CO_2 and N_2 in both flames is primarily thermal. The reaction zone temperature in the flame-anchoring region of the heptane flame at extinction agrees well with the adiabatic flame temperature corresponding to the lean flammability limit. In propane flame, where the flame base is lifted off the burner before extinction, the reaction zone temperature at extinction is 100–200 K higher than the adiabatic flame temperature at the lean flammability limit.

Introduction

WITH recent aircraft accidents attributed to fire-related causes, and because of demands to develop alternatives to Halons, the interest in fire extinguishment has been reinvigorated. Several materials have been identified as possible substitutes for CF_3Br . Some of them have been tested for their effectiveness in laboratory-scale apparatus. These studies include mixing extinguishing agents in air flowing concurrently with or counter to the direction of fuel streams.¹ The mechanisms of fire extinction² and scaling effects³ have also been studied. Lott et al.⁴ described a study of the extinguishment effectiveness and the synergism of CO_2 , N_2 , and Halon 1301 in a coflow apparatus similar to the National Fire Protection Association (NFPA) recommended cup burner apparatus,⁵ using heptane. Liquid pool flames are buoyancy controlled, and their burning rate depends primarily on the energy feedback rate to the pool from the flame itself. The extinguishment process in the coflow burner apparatus involves the following steps: 1) diffusion of the extinguishing agent from the coflowing air into the reaction zone located at the interfacial region of fuel jet and airstreams; 2) reduction of reaction rate either through lowering temperature by heat abstraction (thermal) or suppression of chain carrier concentrations (chemical); 3) changes in flame height and soot formation, and accompanying changes in radiation emission; and 4) reduction of fuel evaporation rate that results from the diminished radiative feedback to the liquid surface. The progressive reduction of the burning rate eventually causes flame extinction. The aforementioned steps depend strongly on the chemical structure, sooting, and radiative characteristics of the fuel. Hence, the applicability of extinguishment results obtained in liquid fuel tests to situations such as gas-fed fires, where the fuel feed rate is independent

of the flame characteristics, is questionable. Furthermore, if the fuel feed rate to the reaction zone is decoupled from the characteristics of the ensuing flame, a large part of the complexity in interpreting test results will be circumvented. Hence, this study was conducted to understand 1) the differences in the flame structure of the buoyancy-dominated gas and liquid fuel flames, and 2) the effects of adding physical agents (N_2 and CO_2) to the surroundings on the extinguishment of gas and liquid flames.

Experimental Apparatus and Procedure

The experimental facility consisted of a coflow burner apparatus designed following the NFPA 2001 standards,⁵ and hence, only a brief description is given here. The apparatus shown in Fig. 1 consisted of a 8.5 cm i.d. and 100 cm tall vertically mounted Pyrex® glass chimney. At the base of the chimney a flow distributor containing lead shots 3 mm in diameter was provided. Air was supplied from a compressor through a calibrated rotameter to provide the coflow stream. The extinguishing agents, metered by calibrated rotameters, were mixed with the airstream at the desired concentrations. The agent/air mixture was passed through a large tank (1.5 l) and a flow distributor, and hence, was thoroughly mixed. A cup burner of i.d. 2.15 cm was located concentrically in the chimney, such that the burner rim was 30.5 cm below the exit plane of the chimney. Liquid heptane was supplied to the cup burner from a flask functioning as a self-maintaining constant level device. The liquid level in the cup burner was set at the rim level by adjusting the elevation of the flask. Alternatively, gaseous propane was fed to this burner from a gas cylinder through a pressure regulator and a calibrated rotameter. Steel wool, placed in the cup, provided a uniform distribution of fuel flow at the exit of the burner. An access hole was provided on the side of the Pyrex glass chimney to ignite the fuel with a match. The exhaust from the chimney was vented through an induced draft fan.

Air flow rate in the coflow stream was maintained at 40 l/min, yielding a nominal velocity of 12 cm/s. This flow rate was chosen because it fell in a range where the burning rate of the liquid pool had been found to be insensitive to the changes in the flow rate caused by the addition of extinguishing agents.⁵ Furthermore, this flow rate provided more than seven times the air required for stoichiometric combustion of propane (or four times in the case of heptane). The mass burn-

Received May 5, 1997; revision received Feb. 22, 1998; accepted for publication Oct. 21, 1998. Copyright © 1998 by S. R. Gollahalli. Published by the American Institute of Aeronautics and Astronautics, Inc., with permission.

*Graduate Student, Combustion and Flame Dynamics Laboratory. Student Member AIAA.

†Lesch Centennial Professor, Combustion and Flame Dynamics Laboratory. Associate Fellow AIAA.

‡George Lynn Cross Professor Emeritus and Hughes Centennial Professor Emeritus, Combustion and Flame Dynamics Laboratory.

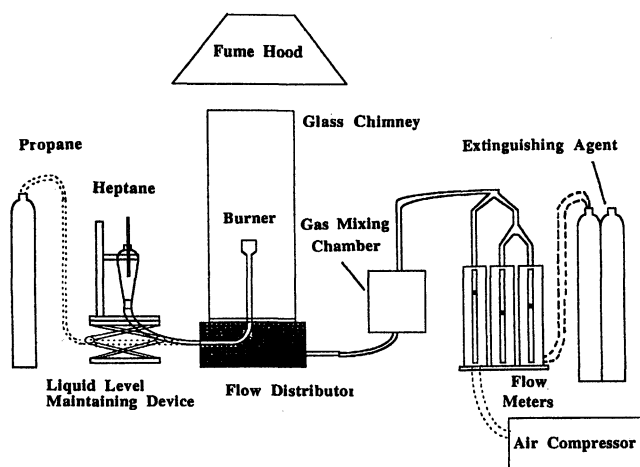


Fig. 1 Experimental apparatus.

ing rate of heptane was determined by continuously weighing the liquid-containing flask with a digital scale. The propane flow rate was adjusted to provide the same velocity at the burner exit as the fuel vapor velocity (1.1 cm/s) in the heptane tests, which was calculated from the results of Lott et al.⁴ At these conditions the flames were laminar with a burner exit Reynolds number of 77 and 53 for heptane and propane flames, respectively (the viscosity of heptane vapor was estimated as 82 μP at the liquid boiling temperature, and that of propane as 80 μP at room temperature). The Froude number (defined as U^2/gd , where U is the mean gas velocity at the burner exit, g is the acceleration caused by gravity, and d is the burner diameter) was 0.0005 for both fuels. Hence, both liquid heptane and gaseous propane flames were buoyancy controlled.⁶

Radial temperature profiles in flames were obtained with a chromel–alumel thermocouple. Because the same thermocouple was used in studies with chemical suppressants, to prevent rapid degradation of the material and consequent effects on the calibration and life of the thermocouple, the hot junction of 0.5 mm diameter was shielded with a closed-end stainless-steel tube. Because the measurements were obtained at nearly steady-state conditions, the thermocouple response time was satisfactory. However, the readings were corrected to account for radiation and conduction losses following Fristrom and Westenberg.⁷ For these calculations, the properties of flame gases were estimated at the measured junction temperature. The emissivity of the hot junction and the sink temperature for radiation correction calculations were assumed to be 0.9 and the measured wall temperature of the chimney. The temperature of gases exiting the chimney was also measured with the same thermocouple. Samples of exhaust gases were withdrawn through a stainless-steel probe (1 mm i.d.), treated to remove moisture and particulates, and analyzed for the volumetric concentrations of CO, CO₂, C₃H₈, and O₂, with nondispersive infrared and polarographic detectors.

The experimental procedure consisted of the following steps: 1) setting heptane level or propane flow rate, 2) setting coflow rate of airstream, 3) increasing the flame-extinguishing agent flow rate slowly by small increments to allow enough time (10 s) for the flow to equilibrate at each condition, 4) noting the conditions at which the flame lifts off, and 5) noting the conditions at which the flame extinguishes. The volumetric concentrations of extinguishing agents in the coflowing air at the instant of flame extinction were calculated from the measured flow rates of air and agents.

The biased errors in concentration measurements were minimized by frequently calibrating the sampling system and instruments with standard gas mixtures. The accuracy of instruments used for the measurements of the concentrations of CO, CO₂, O₂, and C₃H₈, and temperature were 10 ppm, 0.1%, 0.1%,

1%, and 1 K, respectively. With an assumed uncertainty of 5% in the emissivity of the bead and the recorded readability of instruments, the overall spread of the accuracy error propagated into flame temperature is estimated to be 35 K. Each experimental run was repeated 3–5 times and the measure of repeatability was calculated using t distribution. The estimated uncertainties at 95% confidence level in gas temperature and concentrations of CO₂, CO, and O₂ were ± 2 , $\pm 0.2\%$, $\pm 15\%$, and $\pm 0.2\%$, respectively.

Results and Discussion

Flame Appearance and General Observations

Visual observations and photographs⁸ of heptane and propane flames in a pure airstream, and in airstreams containing 50 and 95% of the agent (CO₂ or N₂) concentration required for extinction, reveal the following facts. The changes in flame appearance are qualitatively similar for CO₂ or N₂ addition. In a pure airstream, heptane flame has a small blue region (~ 3 mm long) at the rim of the cup. The core of the flame near the burner consists of a dark region where fuel pyrolysis and soot formation reactions occur. A long luminous yellow region follows the blue region. With an increase in the concentration of an extinguishing agent in the coflow stream, the lengths of the blue and dark regions increase, whereas the length and luminosity of the yellow region decrease. The flame becomes less steady and begins to flicker. As the point of extinction is approached, the flame base wanders around the rim and eventually becomes extinct. Although similar changes occur in propane flames, flame extinction is preceded by the lifting of the flame base off the burner rim. The luminosity decreases by a much larger extent.

The small bluish region near the rim of the heptane and propane flames is attributed to the premixed flame of fuel vapor and air diffused into the flame quench region near the burner. This premixed flame region is also responsible for anchoring the flame. The yellow color is caused by the emission from burning soot particles formed by the pyrolysis of fuel. As the concentration of the extinguishing agent in the coflow stream increases, the flame color changes to blue, and the accompanying reduction in luminosity leads to a decrease in the rate of energy feedback to the liquid surface and fuel evaporation rate. These factors cause the flame to wander around the rim. The preceding processes rapidly build up and extinguish the flame. The larger decrease in flame luminosity in the case of propane is caused by the additional air entrainment over the lift-off height into the soot formation region, which lowers the amount of soot burning downstream.

Mass Burning Rate

Figure 2 shows the mass burning rates of heptane pool as a function of CO₂ and N₂ concentrations in air. The values of burning rate are in the range quoted in the literature.^{9,10} As the concentration of the agent is increased, the burning rate decreases in conformity with the visual observations, as discussed earlier. In propane flame experiments, the fuel feed rate

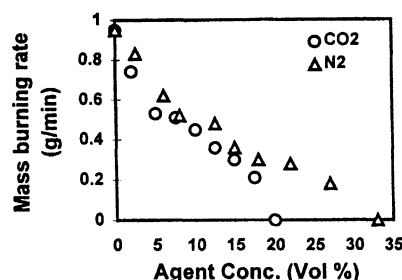


Fig. 2 Effects of additional CO₂ and N₂ in a coflow airstream on the mass burning rate in heptane flame. Experimental uncertainty in mass burning rate at 95% confidence is within $\pm 1\%$ of the mean values shown.

was externally controlled and maintained at 235 ml/min until extinction.

Extinction Concentration of Agents

It is noted from Fig. 2 that the concentrations of additional N_2 and CO_2 in the coflow airstream at the point of extinction of heptane flames were 33 and 20% (by volume), respectively, confirming that CO_2 was more effective than N_2 . In propane flames, within the experimental uncertainty, the extinction concentrations of N_2 and CO_2 were the same as in heptane experiments. Trees et al.¹ reported N_2 extinguishment results in a similar coflow apparatus with heptane and propane flames. Their results closely agree with the present results of N_2 concentration at extinction (33%), and in the lack of any significant differences in its value between propane and heptane flames. It is to be noted that propane flame lifts off the burner at volumetric concentrations of 23% and 15% of additional N_2 and CO_2 , respectively.

Temperature Profiles

Flame Anchoring Region

Figure 3 shows radial temperature profiles in the bluish flame base region ($x/d = 0.23$) and in the luminous yellow region ($x = 0.67L$, where L is the visible flame length), in heptane flames burning in pure air, and in air mixed with nitrogen at 50 and 95% of the concentration required to cause extinction. Figure 4 shows the corresponding temperature profiles when CO_2 was mixed with air. Figures 5 and 6 show the data in propane flames.

In the near-nozzle region of both heptane and propane flames, a double-hump structure in the temperature profiles, characteristic of diffusion-controlled interface combustion, is seen. In the far-nozzle region of heptane flames, these peaks

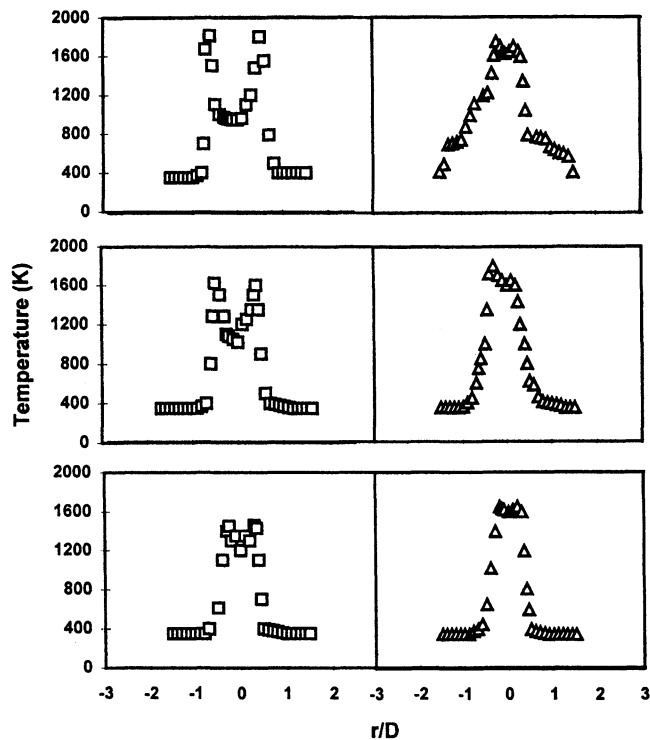


Fig. 3 Radial temperature profiles in heptane flames with the addition of N_2 to the coflow stream (left: near-nozzle region, $x/d = 0.23$; right: far-nozzle region, $x = 0.67$ visible flame length L). Top: coflow = air, $L = 28$ cm; middle: coflow = air with 50% of additional N_2 concentration at which extinction occurs, $L = 21$ cm; and bottom: coflow = air with 95% of additional N_2 concentration at which extinction occurs, $L = 9$ cm. Experimental uncertainty in temperature at 95% confidence is within $\pm 2\%$ of the mean values shown.

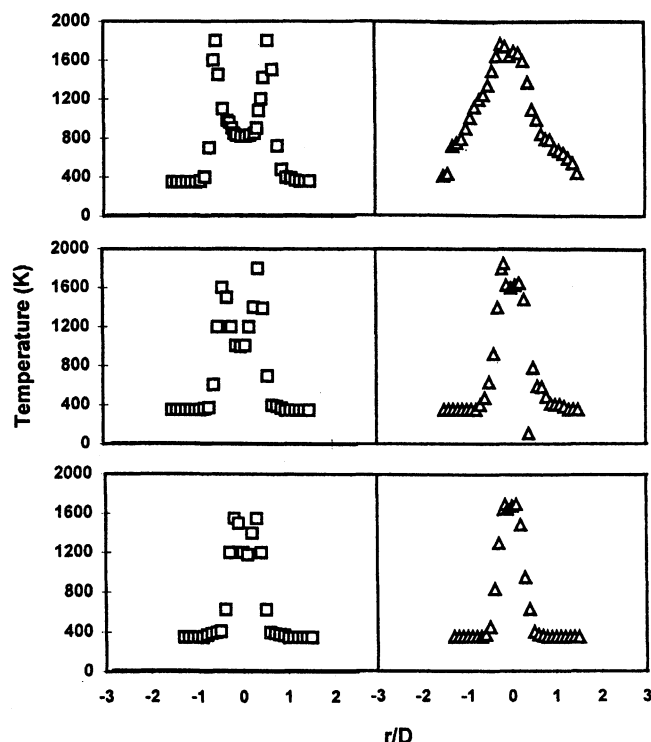


Fig. 4 Radial temperature profiles in heptane flames with the addition of CO_2 to the coflow stream (left: near-nozzle region, $x/d = 0.23$; and right: far-nozzle region, $x = 0.67$ visible flame length L). Top: coflow = air, $L = 28$ cm; middle: coflow = air with 50% of additional CO_2 concentration at which extinction occurs, $L = 16.5$ cm; and bottom: coflow = air with 95% of additional CO_2 concentration at which extinction occurs, $L = 8$ cm. Experimental uncertainty in temperature at 95% confidence is within $\pm 2\%$ of the mean values shown.

become less prominent, whereas in the propane flame only a single axial peak is found. Because soot combustion, controlled by chemical kinetics, is dominant in the far-nozzle region, the double-hump structure becomes less prominent and turns into a single axial peak structure. The peak values of temperature in the flame-stabilization region of heptane and propane flames in pure airstream and in air mixed with flame-suppressing agents (N_2 and CO_2), close to their extinction concentration (95%), are shown in Table 1.

The peak values of temperature in the near-nozzle region of both heptane and propane flames are lower than their adiabatic flame temperature calculated at stoichiometric conditions (STANJAN¹¹). The lower measured values are attributed to the nonadiabaticity of the actual flames and the limited spatial resolution of the thermocouple probe in recording the peak values. The trends of temperature variation are interesting. It is seen that the peak values decrease with the increase in extinguishing agent concentration. At the agent concentration close to extinction, the peak temperature in heptane flames is approximately equal to 1500 K for both N_2 and CO_2 additions. This suggests that there is a minimum peak temperature in the flame-anchoring region, below which flame cannot be sustained, and that minimum temperature is independent of the physical agent. The flame is anchored at the location where the local gas velocity and the laminar flame velocity corresponding to the mixture formed by the fuel and air diffused into the quench-region on the burner.¹² Hence, at the extinction condition, the mixture condition at the flame anchoring point may be considered to correspond to the lean flammability limit. It is also interesting to note that the adiabatic equilibrium flame temperature at the lean flammability limit (equivalence ratio = 0.53) for heptane is approximately equal to 1500 K, which is the measured peak value of temperature in the stabilization region of heptane flame for both extinguishing agents.

In the propane flame close to extinction, the near-nozzle peak temperature for CO_2 and N_2 addition differs by approximately 100 K. This temperature not only depends upon the agent, but is also higher than the calculated adiabatic equilibrium flame temperature corresponding to the lean flammability limit (equivalence ratio = 0.51) for propane. It should be noted that propane flame is lifted off the burner before extinction, and hence, extinction is caused by the flame blowout, a mechanism that is significantly different from the mechanism of extinction achieved by thermal quenching.

Ewing et al.² calculated the so-called limiting temperatures of heptane flames. Their calculations are supposed to account for all of the heat sinks introduced by the agents, viz., sensible heat, heat of decomposition, dissociation, or vaporization. This value for N_2 and CO_2 is 1877 and 1875 K, respectively. Comparing these values with the equilibrium adiabatic flame temperatures at stoichiometric conditions in air containing 95% of the extinction concentrations of N_2 and CO_2 , we find that the latter are higher. However, in spite of the differences in ab-

solute magnitudes, the drop in peak temperature from the pure-air value to extinction condition is in the neighborhood of 400 K. The temperatures calculated by Ewing et al. are different from the corresponding temperatures at the lean-flammability limit. It appears that the temperature measured at extinction in the flame anchoring region with physical agents agrees with the latter.

Far-Burner Region

The peak temperatures in the luminous region of propane and heptane flames in pure air (Figs. 3–6) are generally lower than those in the flame-anchoring region because of the higher radiant loss caused by burning soot. However, as the extinguishing agent concentration is increased, the peak temperatures in the far-burner region approach the peak values in the flame-anchoring region. As discussed previously, the flames become less sooty with the increase in the extinguishing agent concentration; hence, the differences between the thermal structure of near-burner regions and far-burner regions become

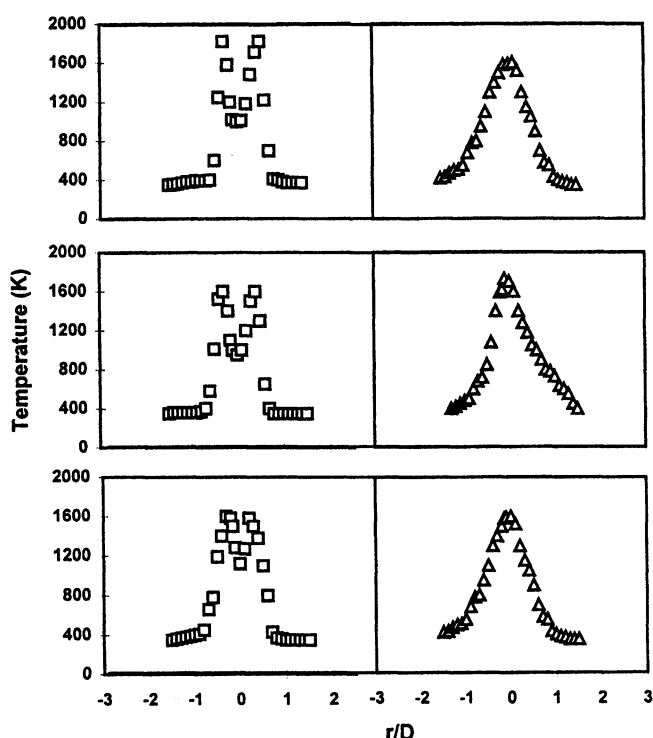


Fig. 5 Radial temperature profiles in propane flames with the addition of N_2 to the coflow stream (left: near-nozzle region, $x/d = 0.23$; and right: far-nozzle region, $x = 0.67$ visible flame length L). Top: coflow = air, $L = 19$ cm; middle: coflow = air with 50% of additional N_2 concentration at which extinction occurs, $L = 18.5$ cm; and bottom: coflow = air with 95% of additional N_2 concentration at which extinction occurs, $L = 15$ cm. Experimental uncertainty in temperature at 95% confidence is within $\pm 2\%$ of the mean values shown.

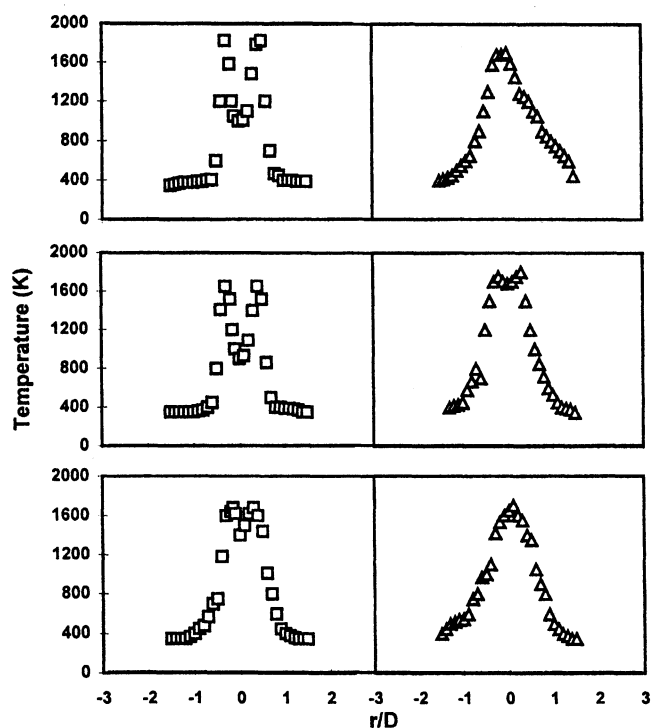


Fig. 6 Radial temperature profiles in propane flames with the addition of CO_2 to the coflow stream (left: near-nozzle region, $x/d = 0.23$; right: far-nozzle region, $x = 0.67$ visible flame length L). Top: coflow = air, $L = 19$ cm; middle: coflow = air with 50% of additional CO_2 concentration at which extinction occurs, $L = 18.8$ cm; and bottom: coflow = air with 95% of additional CO_2 concentration at which extinction occurs, $L = 13$ cm. Experimental uncertainty in temperature at 95% confidence is within $\pm 2\%$ of the mean values shown.

Table 1 Comparison of measured peak temperatures in the near-burner region with calculated adiabatic equilibrium temperature

Fuel	Surrounding environment	Measured peak temperature, ^a K	Adiabatic flame temperature, ^b K
Heptane	Air	1850	2274
	Extinction ^c with N_2	1500	1864
	Extinction ^c with CO_2	1500	2100
Propane	Air	1850	2266
	Extinction ^c with N_2	1600	1929
	Extinction ^c with CO_2	1700	1953

^aIn the flame stabilization (near-burner) region.

^bAt stoichiometric equilibrium conditions.

^cAt 95% of the volumetric concentration of the agent at which extinction occurs.

less prominent. The peak temperature in the far-burner region close to extinction conditions is in the range of 1600–1700 K for both heptane and propane fuels, and when both N_2 and CO_2 were used as extinguishing agents. Because the far-burner region is mainly dominated by soot combustion, and the radical pool generated by fuel pyrolysis is already depleted, the lack of significant difference in temperatures is not surprising. Because of the dominance of heterogeneous chemical kinetics in the far-burner region, which is not accounted by the computer code, no comparisons are drawn between the calculated and measured values of temperature in this region.

Exhaust Temperature

Figure 7 is a plot of exhaust gas temperature measured at the end of the chimney with the extinguishing agent concentration in heptane and propane flames. It is noted that the exhaust gas temperature is about 150 K higher for heptane flame than for propane flame while both were burning in pure air. The difference may be attributed to the differences in energy input rate into the system between the two cases. Because the propane flow rate was adjusted to match the volumetric flow rate of heptane vapor from the pool surface, the higher molecular weight of heptane accounts for the higher energy release rate by ~ 2.3 times than in the case of propane. However, the higher radiant heat loss rate caused by the higher soot concentration in heptane flame compensates for some of the increase of temperature. It is interesting to note that in heptane flame, the exhaust temperature falls continuously with the increase in agent concentration from 700 K in a pure air to 400 K at the instant of extinction. The decrease in exhaust temperature can be accounted for by the decrease in the burning rate of heptane with the increase in extinguishing agent concentration. The exhaust temperature at extinction also seems to be the same for both CO_2 and N_2 , which is in conformity with the behavior of near-nozzle peak temperature at extinction. On the contrary, the variation in exhaust temperature with the extinguishing agent concentration is negligible in the case of the propane flame, primarily because of the constant fuel feed rate to the burner. When the exhaust temperature rise is corrected for the excess air supplied over the stoichiometric amount required to burn the fuel mass (Fig. 2) in pure air or at the extinction condition, the measured temperature at the reaction zone agrees within 100 K with the values calculated for the reaction zone.

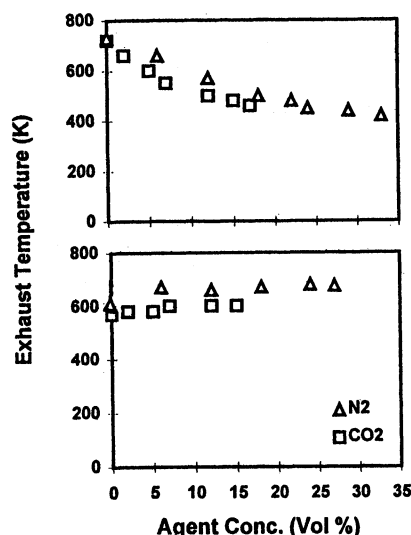


Fig. 7 Effects of additional CO_2 and N_2 in coflow airstream on the exhaust temperature in heptane (top) and propane (bottom) flames. Experimental uncertainty in temperature at 95% confidence is within $\pm 2\%$ of the mean values shown.

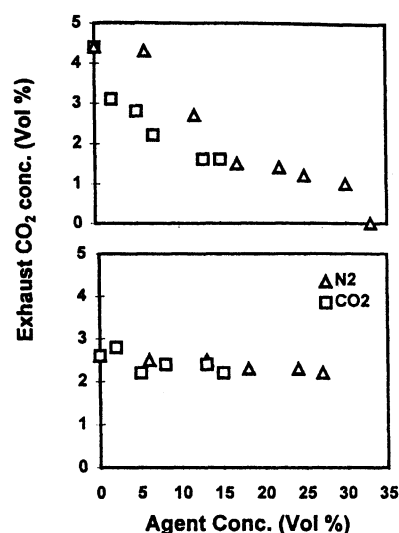


Fig. 8 Effects of additional CO_2 and N_2 in coflow airstream on the exhaust concentration of combustion-generated CO_2 in heptane (top) and propane (bottom) flames. Experimental uncertainty in CO_2 concentration at 95% confidence is within $\pm 0.2\%$ of the mean values shown.

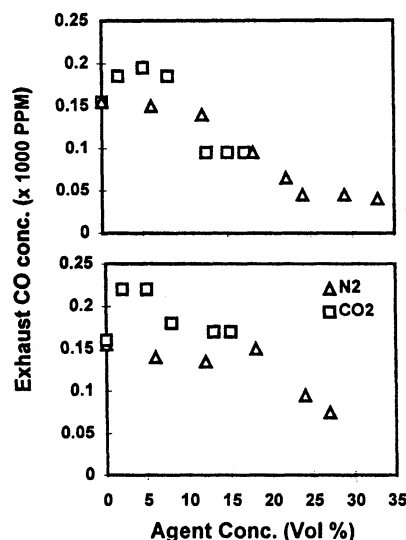


Fig. 9 Effects of additional CO_2 and N_2 in coflow airstream on the exhaust concentration of CO in heptane (top) and propane (bottom) flames. Experimental uncertainty in CO concentration at 95% confidence is within $\pm 15\%$ of the mean values shown.

Exhaust Composition

Figures 8–10 show the variations of CO_2 , CO, and O_2 concentration in the exhaust with the extinguishing agent concentration in heptane and propane flames. The measured concentrations of CO_2 are adjusted to account for the amount of CO_2 supplied, thereby isolating only the combustion-generated CO_2 . It is interesting to note that the combustion-generated CO_2 concentration falls monotonically with the amount of extinguishing agent supplied in heptane flames, by a factor of 4 at extinction. However, its decrease is very small in propane flame. Again, the rapid decline of the burning rate (Fig. 2) in heptane flame and the constant fuel feed rate in propane flame account for a major part of this result. A decrease of exhaust CO_2 concentration, albeit small, in propane flame suggests that combustion efficiency decreases with the increase of extinguishing agent concentration. Hence, it appears that the extinguishing agents, in addition to pure thermal abstraction, affect the chemical reaction process via reduction in concentration of

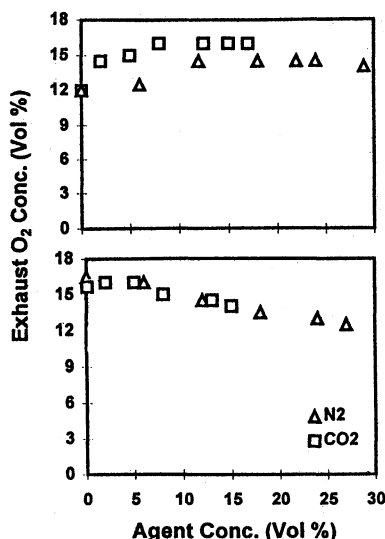


Fig. 10 Effects of additional CO_2 and N_2 in coflow airstream on the exhaust concentration of O_2 in heptane (top) and propane (bottom) flames. Experimental uncertainty in O_2 concentration at 95% confidence is within $\pm 0.2\%$ of the mean values shown.

the reacting species and the reaction temperature. The effect, however, is small.

CO concentration also shows a decrease with the increase in the extinguishing agent concentration in both heptane and propane flames, although a small initial increase is seen with CO_2 in both flames. The initial increase is perhaps a result of the dissociation of the CO_2 added, which becomes negligible as the peak temperature begins to drop. The subsequent decrease in CO may be attributed to a reduction in soot formation and its burning rate, as discussed earlier.

Oxygen concentration in the exhaust is an inverse indication of combustion efficiency. It is interesting to note that in heptane flames, O_2 concentration increases, whereas in propane flames it decreases with the extinguishing agent concentration. The increase of O_2 concentration in heptane flame is evidently a result of the fall in evaporation and the burning rates of fuel, and because of less combustion-generated CO_2 . In propane flame, where the fuel feed rate was kept constant, O_2 concentration falls with the increase of extinguishing agent concentration caused by 1) a better utilization of oxygen in the premixed flame-base accompanying flame liftoff, and 2) the increase in the agent concentration in the coflow stream. The fact that both CO_2 and CO concentrations in exhaust decrease indicates that the second factor is dominant.

Conclusions

The extinction processes of liquid pool and gaseous fuel flames are markedly different, even when both are buoyancy dominated. The differences are expected to be higher between the momentum-dominated gas jet flames and buoyancy-dominated liquid pools. The extinction process in gas flames, except in very small burners, is usually preceded by flame liftoff, which changes the flame structure before extinction. In liquid flames, extinction occurs at the burner rim itself and is preceded by a significant drop in burning rate.

The concentration of CO_2 or N_2 required for extinction is approximately the same in both heptane and propane flames,

in spite of the difference in the flame structure preceding the extinction. Because the adiabatic flame temperatures of these fuels are approximately the same and the extinction limiting temperatures of CO_2 and N_2 are close to each other, it follows that the extinction mechanism of CO_2 and N_2 are primarily thermal. Further, the fact that CO_2 concentration at extinction is smaller than that of nitrogen, reinforces that the heat abstraction effect is the dominant mode of action. The differences in the temperature of the reaction zone required to cause extinction, calculated assuming chemical equilibrium, agree well with the differences in the measured peak temperature in the flame stabilization zone. The peak temperature of the reaction zone estimated from the measured exhaust gas temperature by accounting for the excess air also corresponds adequately to the measured values. The measured peak temperature in the flame stabilization at extinction agrees with the equilibrium flame temperature corresponding to the lean flammability limit of the fuel and is independent of the extinguishing agent. The values calculated assuming equilibrium corresponding to the measured extinguishant concentrations and the limit temperatures given by Ewing et al.² are higher than the measured peak temperature.

Acknowledgment

The authors thank the U.S. Navy for the partial support for this study through Contract N00014-95-1-0525.

References

1. Trees, D., Sheshadri, K., and Hamins, A., "Experimental Studies of Diffusion Flame Extinction with Halogenated and Inert Fire Suppressants," *Halon Replacements*, edited by A. W. Miziolek and W. Tsang, ACS Symposium Series 611, American Chemical Society, Washington, DC, 1995, pp. 190–203.
2. Ewing, C. T., Beyler, C. L., and Carhart, H. N., "Extinguishment of Class B Flames by Thermal Mechanisms; Principles Underlying a Comprehensive Theory: Prediction of Flame Extinguishing Effectiveness," *Journal of Fire Protection Engineer*, Vol. 6, No. 1, 1994, pp. 23–54.
3. Saso, Y., Saito, N., and Iwata, Y., "Scale Effect of Cup Burner on Flame Extinguishing Concentrations," *Fire Technology*, Vol. 29, No. 1, 1993, pp. 22–33.
4. Lott, J. L., Christian, S. D., Sliepcevich, C. M., and Tucker, E., "Synergism Between Chemical and Physical Fire-Suppressants," *Fire Technology*, Vol. 32, No. 3, 1996, pp. 260–271.
5. Anon., *NFPA 2001 Standards on Clean Agent Fire Extinguishing Systems*, 1994 ed., National Fire Protection Association, Quincy, MA, Jan. 1994.
6. Drysdale, D., *An Introduction to Fire Dynamics*, Wiley, New York, 1985.
7. Fristrom, R. M., and Westenberg, A. A., *Flame Structure*, McGraw-Hill, New York, 1965.
8. Babb, M. L., "Extinguishment Characteristics of Gaseous Propane and Liquid Heptane Diffusion Flames in Air," M.S. Thesis, School of Aerospace and Mechanical Engineering, Univ. of Oklahoma, Norman, OK, 1996.
9. Blinov, V. I., and Khudiakov, G. N., "Certain Laws Governing Diffusive Burning of Liquids," *Academica Nauk, SSSR Doklady*, Vol. 113, 1957, pp. 1094–1099.
10. Corlett, R. C., and Fu, T. T., "Some Recent Experiments with Pool Fires," *Pyrodynamics*, Vol. 4, 1966, pp. 253–259.
11. Reynolds, W. C., "The Element Potential Method for Equilibrium Analysis: Implementation in the Interactive Program STANJAN," Version 3, Stanford Univ., Stanford, CA, Jan. 1986.
12. Takahashi, F., Mizomoto, M., Ikai, S., and Futaki, N., "Lifting Mechanism of Free Jet Diffusion Flames," *20th Symposium (International) on Combustion*, The Combustion Inst., Pittsburgh, PA, 1984, pp. 295–302.